



Title	Analysis of Vibration Response Law of Multistory Building under Tunnel Blasting Loads
Author(s)	Huo, Runke; Li, Shuguang; Song, Zhanping; Fujii, Yoshiaki; Lei, Shan; Mao, Jianchao; Tian, Sisi; Miao, Zizhen
Citation	Advances in Civil Engineering, 2019, 1-16 <a href="https://doi.org/10.1155/2019/4203137">https://doi.org/10.1155/2019/4203137</a>
Issue Date	2019-02-17
Doc URL	<a href="http://hdl.handle.net/2115/72505">http://hdl.handle.net/2115/72505</a>
Rights(URL)	<a href="https://creativecommons.org/licenses/by/4.0/">https://creativecommons.org/licenses/by/4.0/</a>
Type	article
File Information	AdvancesInCivilEngineering_Vol2019ArticleID4203137.pdf



[Instructions for use](#)

## Research Article

# Analysis of Vibration Response Law of Multistory Building under Tunnel Blasting Loads

Runke Huo <sup>1</sup>, Shuguang Li <sup>1,2</sup>, Zhanping Song <sup>1,3</sup>, Yoshiaki Fujii <sup>2</sup>, Shan Lei,<sup>4</sup>  
Jianchao Mao,<sup>1,3</sup> Sisi Tian,<sup>1,3</sup> and Zizhen Miao<sup>5</sup>

<sup>1</sup>School of Civil Engineering, Xi'an University of Architecture and Technology, Xi'an 710055, China

<sup>2</sup>Rock Mechanics Laboratory, Faculty of Engineering, Hokkaido University, Sapporo 060-8628, Japan

<sup>3</sup>Institute of Tunnel and Underground Structure Engineering, Xi'an University of Architecture and Technology, Xi'an 710055, China

<sup>4</sup>Department of Remote Sensing Engineering, Henan College of Surveying and Mapping, Zhengzhou 451464, China

<sup>5</sup>Beijing No. 4 Municipal Construction Engineering Co. Ltd., Beijing 100176, China

Correspondence should be addressed to Shuguang Li; [lssgg2015@163.com](mailto:lssgg2015@163.com) and Zhanping Song; [songzhp@xauat.edu.cn](mailto:songzhp@xauat.edu.cn)

Received 7 November 2018; Accepted 13 January 2019; Published 17 February 2019

Academic Editor: Dong-Sheng Jeng

Copyright © 2019 Runke Huo et al. This is an open access article distributed under the Creative Commons Attribution License, which permits unrestricted use, distribution, and reproduction in any medium, provided the original work is properly cited.

This paper takes the Dizong tunnel engineering as its background. Combined with the on-site monitoring data, the wavelet packet program based on MATLAB was compiled to study the vibration response of the four-story masonry building in a typical southwestern mountainous area of China under the blasting load. The results showed that the maximum particle velocity increased to the 3rd floor and attenuation occurred on the 4th floor. The particle velocity in the z-direction was the largest and should be paid attention. The dominant frequency of the building showed a trend from high frequency to low frequency, the duration became short, and the acceleration decreased to the 4th floor. With the increase of the building floor, the main frequency domain of the building decreased and then gradually tended to the low-frequency domain. The high-frequency particle velocity gradually decreased, gathered to the low frequency, and developed from the dispersed multiband to the concentrated low-frequency band. The total energy value of vibration increased to the 3rd floor and then decreased to the 4th floor. The energy of the building was between 0 and 171.6 Hz. The higher the floor was, the more concentrated the energy was in the low-frequency domain.

## 1. Introduction

In recent years, many researches on the response of buildings under blasting load by tunnel construction have been conducted. Dowding et al. [1] studied the response law of old multistory houses under high-frequency rock blasting. The results showed that close-range rock blasting exerted short-wavelength excitation on building and cannot simultaneously stimulate large structures. Ma et al. [2] monitored the vibration velocity of the surface particles after the auxiliary hole blasting at the channel No. 1 of Yan'an Road Station of Qingdao Metro Line 2 and obtained the influence of the blasting cavity on the vibration response of

the building. Yang et al. [3] compared the frequency characteristics caused by blasting vibration through a tunnel excavation using a full-section millisecond delay blasting sequence for the first time. The results showed that the frequency of single-delay vibration signal decreased with the size of the equivalent blasting vibration source if the geometrical shape and the charge structure of the blasthole remain constant for each time-delay blasting. Based on a hydraulic tunnel project in Guyuan City, Ningxia, China, Qiao et al. [4] used the field test methods to analyze the blasting vibration frequency and vibration velocity. The safety distance of the adobe house and the brick house was found to be 160 m and 60 m, respectively. Based on the

blasting construction of Qingdao Metro Tunnel, Yuan et al. [5] determined the safety allowable vibration velocity, blasting single hole charge, and construction vibration impact range of different buildings along the Qingdao Metro. Wang et al. [6] analyzed the relationship between the maximum values of the vibration velocity and the floor of the building with the Qingdao terminal connection project of the Jiaozhou Bay submarine tunnel. Based on a large amount of monitoring data, Reza et al. [7] studied the effects of different rock formations, different detonators, and different explosives on the surface movement caused by blasting vibration near the underground and surface concrete structures during the construction of the upper Gotvand dam. Fan et al. [8], Shin et al. [9], Duan et al. [10], and Dang et al. [11] combined numerical simulation and on-site monitoring data to investigate the effects of blasting vibration on the safety of buildings, existing tunnels, buried pipelines, and roadways from the aspects of seismic velocity, blasting seismic waves, and blasting load. Rebello et al. [12], Li et al. [13], Zhang et al. [14], Chen et al. [15], and Guan et al. [16] studied the vibration rate of the building by the tunnel blasting and found that the vertical velocity was the main component. Wang et al. [17] determined the main parameters affecting the vibration spectrum by the K-means method based on a large number of blasting vibration signals. At present, researches on the influence of blasting vibration on buildings mostly focus on vibration velocity. However, the systematic study on the frequency, duration, acceleration, spectrum, and energy characteristics as well as velocity is essential to limit damages of the building.

Based on the Dizong tunnel engineering, in this paper, the spectrum of vibration signals, the maximum vibration velocity with the distribution of the frequency band, and the energy distribution with the frequency band were analyzed by the wavelet packet analysis technology, and the response law of the multilayered masonry building to the blasting vibration at the shallow burial Dizong tunnel was formed based on the MATLAB program. The results were intended to provide a theoretical basis and technical support for the evaluation of building safety under blasting vibration and for the optimization of blasting design.

## 2. Engineering Background

The newly constructed An-Liu high-speed railway is an intercity high-speed railway connecting city of Anshun and Liupanshui, Guizhou, China. The Dizong tunnel is an essential node project of the ALTJ-2 section of the An-Liu high-speed railway station (Figure 1). The two-lane tunnel is 3045 m long and has a 3.6 m wide median strip. According to the standard of the International Tunnel Association, the tunnel belongs to super-large section tunnel ( $105.90 \text{ m}^2 > 100.00 \text{ m}^2$ ). Section DK42 + 200~DK42 + 450 of the tunnel is a shallow buried section with a minimum buried depth of about 12 m, which is the key monitoring section (Figure 2).

The Dizong tunnel passes through the mountainous area of Chashan village. There are 60 households in the section of DK41 + 945~DK42 + 495 with an area of 11061.54 m<sup>2</sup>. The

buildings in these sections are simple and old, on the poor foundations.

## 3. Blasting and Monitoring Schemes

**3.1. Blasting Scheme.** According to the hydrological and geological conditions, the surrounding rock grade, and other conditions, the two-step method was utilized for construction. The single-cycle footage for the upper section was 2.4 m and 3.0 m for the lower section. The YT-28 rock drill with a diameter of 40 mm was used. The explosive used was RJ-2 waterproof emulsion explosive. The diameter of the surrounding blasthole pack was 25 mm, and the diameter of other blasthole packs was 32 mm. The arrangement of the blastholes and the grooves for the upper section is presented in Figure 3, and the blasting design parameters are given in Table 1. The ordinary millisecond detonating industrial No. 8 detonator with 1~15 segments was used in separate sections. The upper step around blasthole spacing was 50 cm, the inner ring blasthole spacing was 120 cm, the vertical blasthole spacing was 20 cm, and the floor blasthole spacing was 100 cm. The smooth blasting technique was used. The peripheral blastholes were taken by noncoupling charge, and the interval component was loaded.

### 3.2. On-Site Monitoring Schemes

**3.2.1. Overview of the Building.** The monitoring house is a self-built residential building in Chashan Village, with a distance of 51.2 m and a vertical distance of 29.8 m from the tunnel face (Figure 4). The house has 4 floors, the height of the 1st and 2nd floors is 3.2 m, the height of the 3rd and 4th floors is 2.8 m, and the floor area is 152 m<sup>2</sup>. The house adopts a masonry concrete structure. The used stone with relatively regular shape were mined by the local people. The construction of the 1st and 2nd floors was early, the masonry blocks were larger, and the 3rd and 4th floors were built later and smaller masonry blocks were used. Concrete mortar was applied on the exterior of the wall (Figure 4).

**3.2.2. Monitoring Scheme.** The corners of the building were selected as the measuring points because they were prone to be damaged due to blasting vibration [18]. The enhanced TC-4850 blasting seismometers developed by the Chengdu Branch of the Chinese Academy of Sciences were used for monitoring. When the tunnel was excavated to DK42 + 430, the seismometer was installed by gypsum at the leftmost corner of each floor of the building. The  $x$  and  $y$  direction of the sensor was perpendicular to the tunnel excavation direction and parallel to the tunnel excavation direction, respectively. The  $z$ -direction was vertical upward (Figures 5 and 6).

## 4. Results and Discussion

**4.1. Main Evaluation Indexes.** The main indicators for evaluating the impact of blasting on buildings are maximum particle velocity, the dominant frequency, duration, and

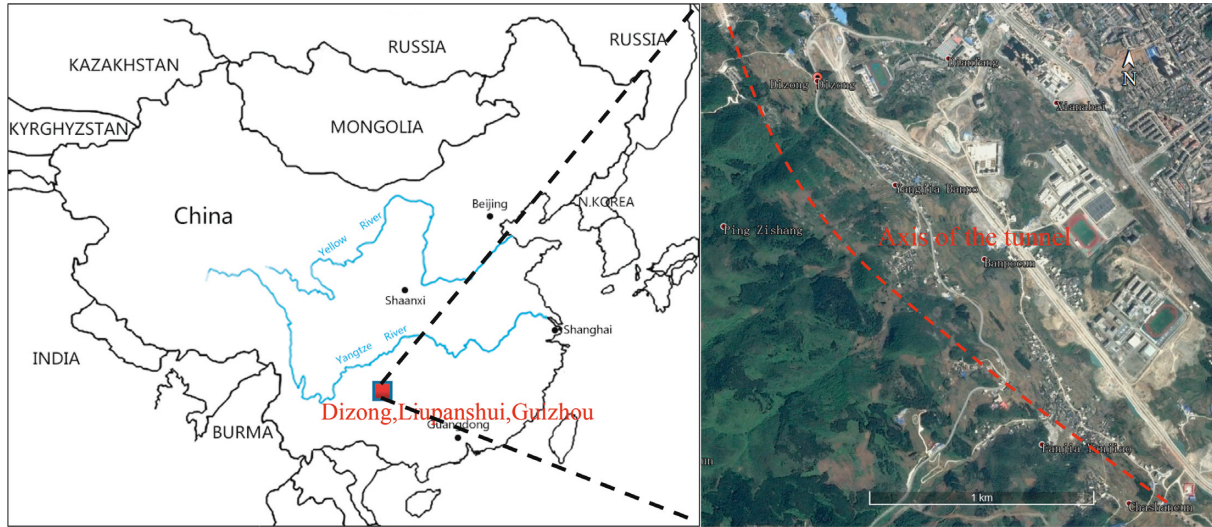


FIGURE 1: Location description of the Dizong tunnel.

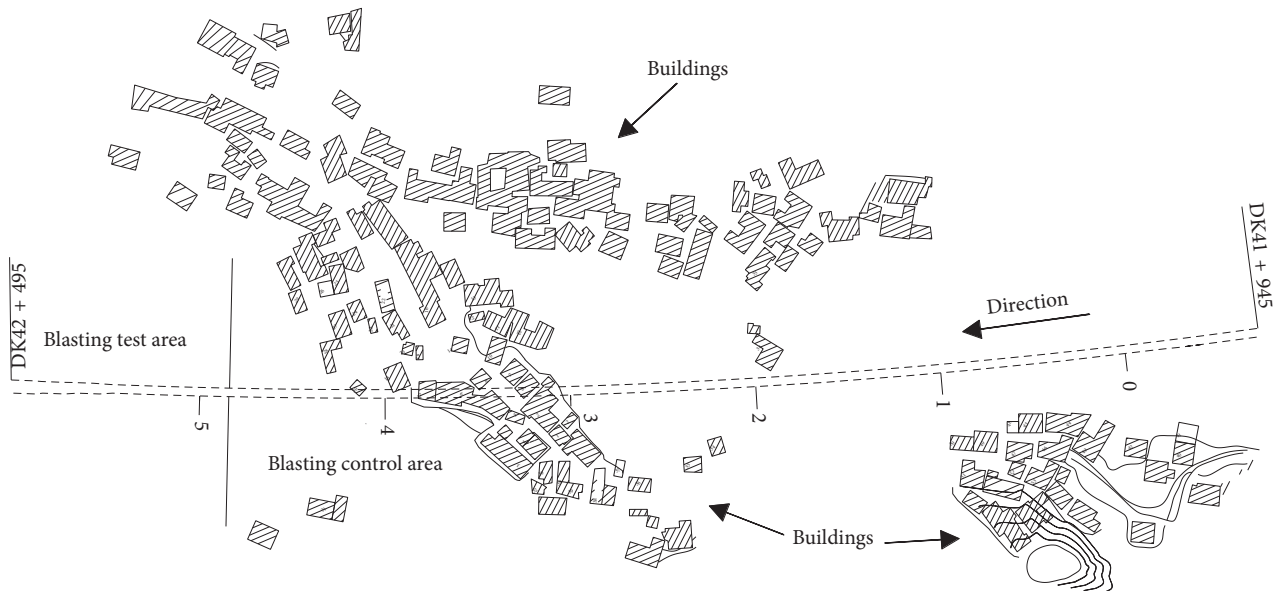


FIGURE 2: The planar view of the tunnel and buildings.

acceleration [19]. According to the above monitoring scheme, the housing response caused by the upper step blasting excavation on the tunnel was monitored four times, and the main evaluation indicators were analyzed based on the monitoring data (Table 2).

**4.1.1. Maximum Particle Velocity.** The maximum particle velocity showed an increasing trend, reaching a maximum value at the third floor, and then decreasing (Figure 7). The combined speed ( $V$ ) was strongly affected by the  $V_{zmax}$ , indicating that  $V_{zmax}$  can better reflect the vibration velocity of the building in the blasting vibration response and the change of  $V_{zmax}$  should be paid more attention during the blasting construction.

**4.1.2. Analysis of the Main Vibration Frequency Change on Different Floors.** The dominant frequency of blasting vibration is an important parameter to characterize the blasting vibration hazard [20].

The overall trend from high frequency to low frequency appeared with the increase in the building floor (Figure 8). The dominant vibration frequency fluctuation in the  $x$ -direction was apparent; the dominant vibration frequency was discrete in the first layer and the third layer, distributed at 33–75 Hz, 26–51 Hz, respectively (Figure 8(a)). The dominant vibration frequency of the  $y$ -direction exhibited a good change law and was relatively concentrated (Figure 8(b)). The distribution of the dominant vibration frequency of the second layer in the  $z$ -direction was relatively discrete, mainly distributed at 50–81 Hz, the dominant vibration frequencies

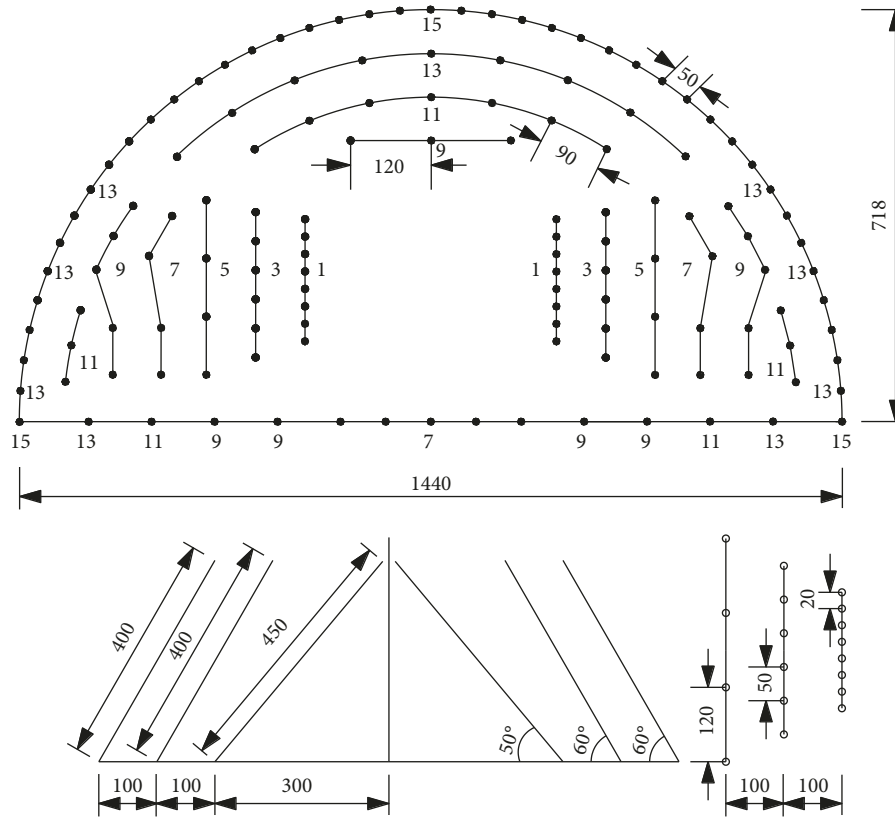


FIGURE 3: Layout of the blasthole and groove for the upper section (Unit: cm).

TABLE 1: Parameters of upper section blasting.

Detonator segment	Hole depth (m)	Hole number	Blasthole name	Explosive charge per hole (kg)	Single-stage charge (kg)
1	3.5	16	Cutting hole	1.5	24
3	2.7	12	Driving hole	1.2	13.4
5	2.7	8	Driving hole	0.9	7.2
7	2.7	8	Driving hole	0.9	11.7
7	2.7	5	Floor hole	0.9	
9	2.7	7	Driving hole	0.9	
9	2.7	6	Inner ring hole	0.9	14.3
9	2.7	4	Floor hole	0.9	
11	2.7	6	Inner ring hole	0.9	
11	2.7	2	Floor hole	0.9	13.5
11	2.7	7	Driving hole	0.9	
13	2.7	8	Around hole (odd)	0.3	
13	2.7	8	Around hole (even)	0.6	
13	2.7	9	Inner ring hole	0.9	17.1
13	2.7	2	Floor hole	0.9	
15	2.7	2	Floor hole	1.2	
15	2.7	12	Around hole (odd)	0.3	13.8
15	2.7	13	Around hole (even)	0.6	
Total	-	135	—	—	117

of other layers were concentrated (Figure 8(c)). When the same or similar peak particle velocity is considered, the dominant vibration frequency of the building became smaller with the increase in the building floor, indicating that the higher the floor of the building was, the more

dangerous it was during the tunnel blasting process. Therefore, in the process of tunnel blasting, the vibration monitoring of high-rise buildings should be strengthened, and the floor of the building should be considered in the vibration evaluation standard.

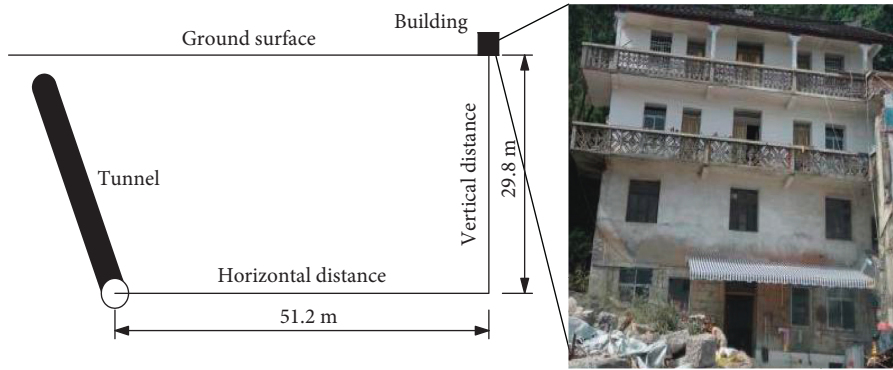


FIGURE 4: The tunnel and the building.

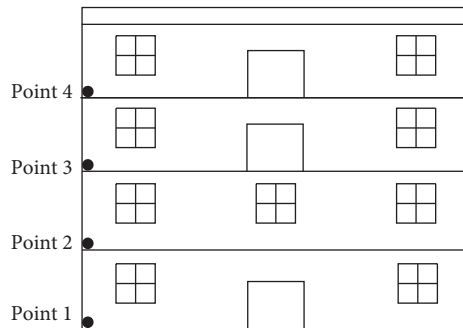


FIGURE 5: Schematic diagram of measuring points.



FIGURE 6: Schematic diagram of instrument installation.

TABLE 2: Raw monitoring data.

Floor	M	$V_{xmax}$	$V_{ymax}$	$V_{zmax}$	$V_{max}$	$F_x$	$F_y$	$F_z$	$D_x$	$D_y$	$D_z$
First	1	0.449	0.479	1.036	1.227	33.6	65.4	68.5	1.260	1.241	1.423
	2	0.359	0.517	0.876	1.079	73.5	68.1	80.6	1.261	1.253	1.453
	3	0.393	0.556	1.109	1.301	45.5	55.2	78.1	1.219	1.245	1.666
	4	0.415	0.427	0.868	1.301	62.0	72.0	75.0	1.230	1.183	1.326
Second	1	0.468	0.570	1.078	1.396	46.3	59.5	80.6	1.207	1.175	1.321
	2	0.440	0.546	1.063	1.274	50.0	58.1	73.5	1.200	1.203	1.240
	3	0.482	0.595	1.231	1.364	53.2	61.0	61.0	1.181	1.143	1.412
	4	0.448	0.510	0.935	1.471	51.0	55.6	50.0	1.200	1.071	1.252
Third	1	0.516	0.752	1.354	1.556	50.0	41.7	44.9	1.141	1.153	1.213
	2	0.540	0.699	1.337	1.602	50.5	39.2	46.3	1.170	1.120	1.193
	3	0.545	0.619	1.429	1.630	42.9	40.7	53.8	1.098	1.128	1.274
	4	0.626	0.555	1.404	1.630	26.6	34.8	53.2	1.109	1.067	1.142
Fourth	1	0.423	0.627	1.061	1.303	19.8	21.7	27.2	1.098	1.096	1.189
	2	0.398	0.512	0.865	1.081	16.1	25.0	26.3	1.160	1.061	1.040
	3	0.446	0.554	0.837	1.099	25.6	20.8	26.3	1.057	1.057	1.121
	4	0.499	0.530	0.892	1.099	20.0	21.7	30.3	1.103	1.017	1.059

Note. M represents the number of monitoring;  $V_{xmax}$ ,  $V_{ymax}$ ,  $V_{zmax}$ , and  $V$  represent the peak particle velocity (cm/s) in x, y, z, and co-direction, respectively;  $F_x$ ,  $F_y$ , and  $F_z$  represent dominant frequency (Hz) in x, y, and z directions, respectively;  $D_x$ ,  $D_y$ , and  $D_z$  represent duration (s) of the vibration in x, y, and z directions, respectively.

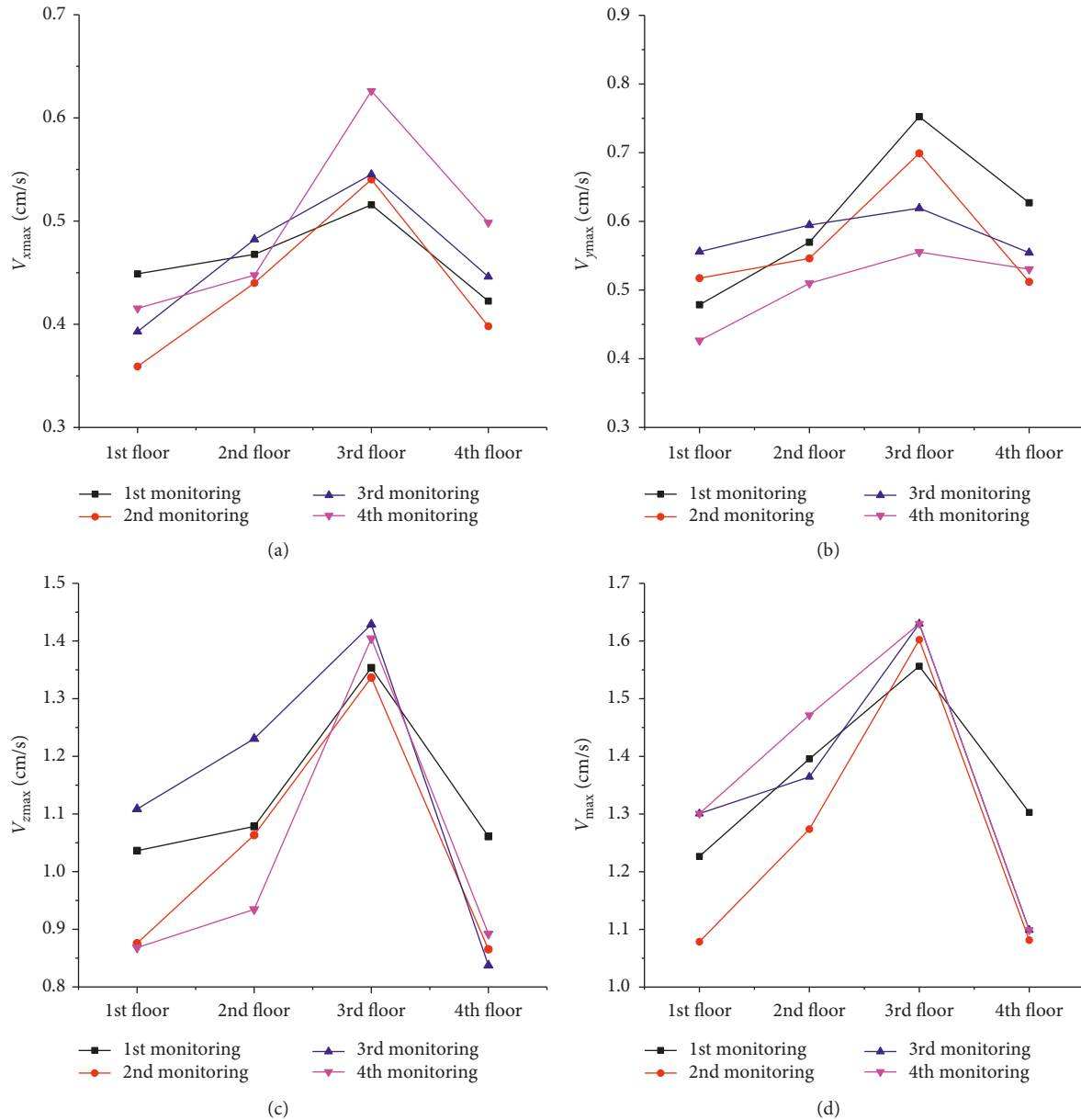


FIGURE 7: Maximum particle velocity: (a)  $V_{xmax}$ ; (b)  $V_{ymax}$ ; (c)  $V_{zmax}$ ; (d)  $V_{max}$ .

4.1.3. *Duration of Vibration.* Figures 9(a)–9(c) show changes of the vibration duration in the  $x$ ,  $y$ , and  $z$  directions with the change of the building floor by four monitoring. It can be seen from Figure 9 that the duration was 1–1.6 s as the floor height increases. In the four monitoring, the vibration duration of the fourth layer in the  $z$ -direction was reduced by 0.23 s, 0.41 s, 0.54 s, and 0.26 s, respectively, compared with the first layer. With the increase of the building floor, the vibration duration decayed in the  $z$ -direction faster than in the  $x$  and  $y$  directions. It is realized that vibration in the  $z$ -direction has a significant influence on the damage of the building.

4.1.4. *Maximum Acceleration.* Figures 10(a)–10(c) show changes of the acceleration in the  $x$ ,  $y$ , and  $z$  directions with

the change of the building floor by four monitoring. It can be seen from Figure 10 that the maximum acceleration decreased with the increase in the number of floor. The maximum acceleration of the fourth layer in the  $z$ -direction was decreased by 69.5%, 54.1%, 68.6%, and 66.6%, respectively, compared with the first layer. With the increase in the building floor, duration decayed in the  $z$ -direction was faster than in the  $x$  and  $y$  directions. The acceleration in the  $z$ -direction was the highest. It is consistent with the analysis above that the  $z$ -direction vibration has a significant influence on the damage to the building.

4.2. *Wavelet Packet Analysis.* The wavelet packet transform can decompose the high and low frequencies of the signal together, so that it can realize the refined analysis of the

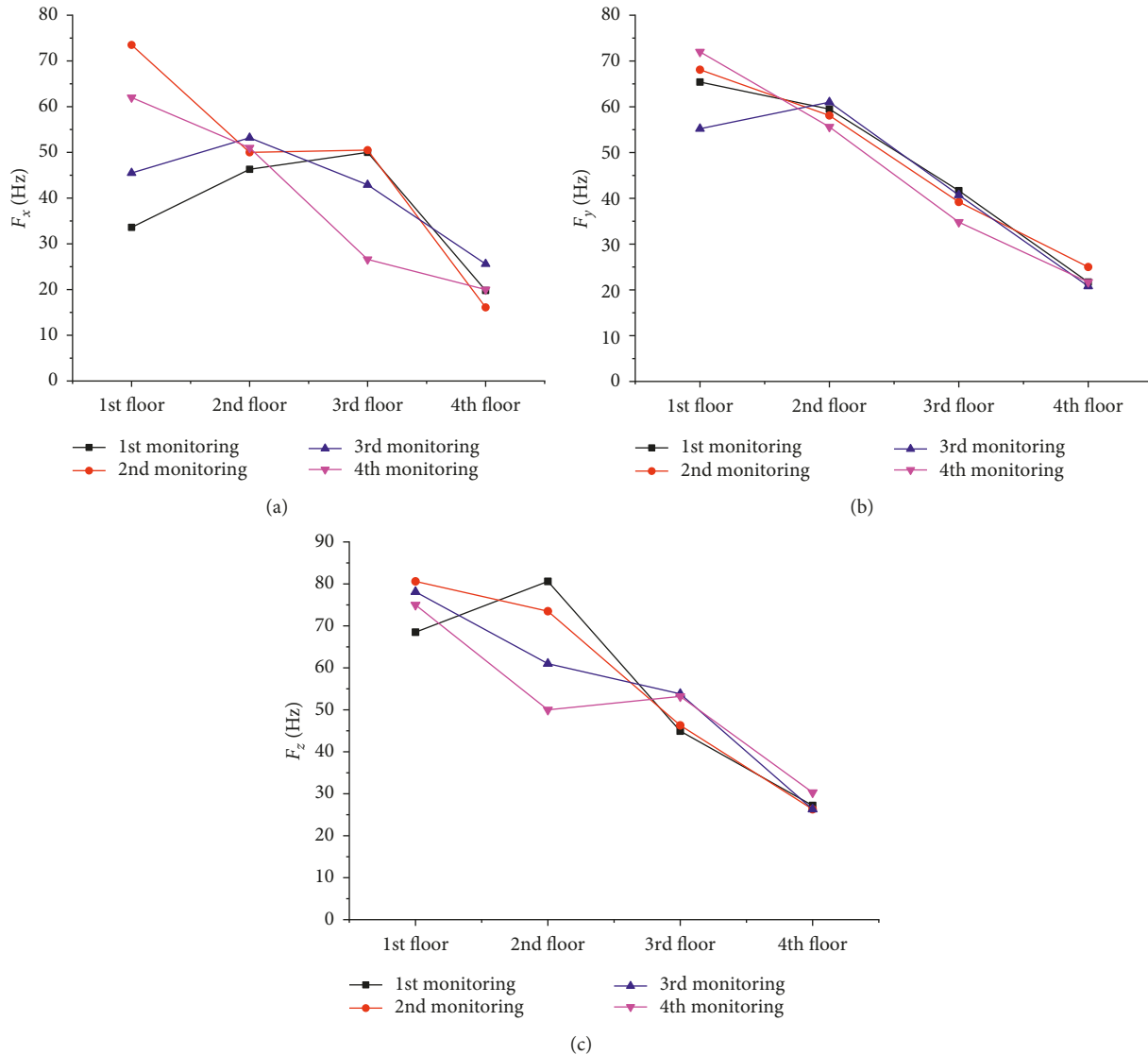


FIGURE 8: Dominant frequency: (a)  $F_x$ ; (b)  $F_y$ ; (c)  $F_z$ .

blasting vibration signal. As a complex system with multiple substructures, the response of the building to the blasting vibration is very complicated. For this reason, the wavelet packet analysis technique can be utilized to refine the vibration response [21].

The program of wavelet packet decomposition and reconstruction was written based on MATLAB software. The db8 wavelet base was utilized to analyze the blasting vibration signal by wavelet packet. The number of decomposition layers was 6 layers. Since the sampling rate was 2000 Hz, according to the sampling law, the Nyquist was 1000 Hz, and the number of decomposition bands was 256 and then each frequency band was 14.6 Hz. Taking the signal in the  $z$ -direction at the first layer in the third monitoring as an example, the original signal data are as shown in Figure 11. After wavelet packet decomposition and reconstruction, the signals of each frequency band can be achieved. The reconstruction data for the frequency bands 1~14 (0~218.4 Hz) are shown in Figure 12.

**4.2.1. Power Spectral Density.** In the blasting engineering, the dominant frequency and the dominant frequency domain are often used to analyze the spectral characteristics of the blasting vibration. After the wavelet packet was decomposed and reconstructed by the wavelet packet, the PSD (power spectral density) of each frequency band can accurately describe the contribution of each frequency band to the blasting vibration, and the spectral characteristics of the signal can be analyzed more precisely [22]. Calculating the PSD of the signals in each frequency band after wavelet packet decomposition and reconstruction (Figure 13), the main frequency domain of the signal can be obtained. The dominant frequency domain and the dominant frequency data of each frequency band are shown in Table 3.

It can be seen from Figure 13 and Table 3 that the main frequency domain of the building became smaller with the increase of the floor and gradually tended to the low-frequency domain. The main frequency domain in the three directions of  $x$ ,  $y$ , and  $z$  was larger in the first layer and

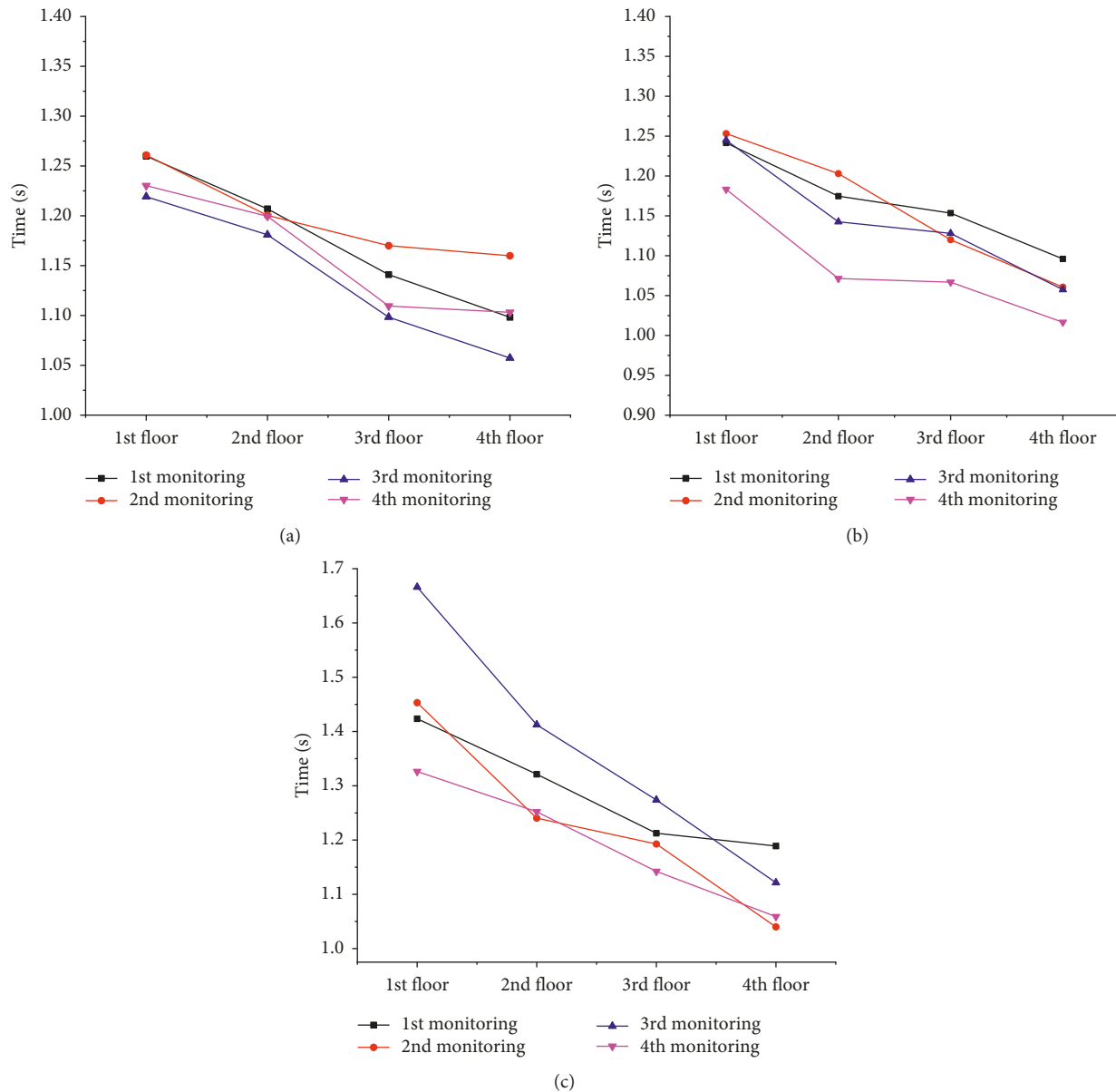


FIGURE 9: Vibration duration: (a) x; (b) y; (c) z.

then reduced to 14.6~46.8 Hz, 0~46.8 Hz, and 0~62.4 Hz, respectively, when it reached the fourth layer. The response signal of the building to blast vibration was widely distributed in the frequency domain, but its main frequency band was basically between 0 and 140 Hz. From the dominant frequency of each frequency band, the dominant frequency of the low-frequency band in the y and z directions was mainly around 14 Hz, but the lower dominant frequency of 1.5 Hz and 2.5 Hz appeared in the low-frequency band in the x-direction, which was very close to the natural vibration frequency of the building and should be paying attention.

4.2.2. Particle Velocity Distribution with respect to the Frequency Band. In most frequency domains, the vibration velocity in the z-direction was the highest, the y-direction was

the second highest, and the x-direction was the lowest (Figure 14). With the increase in the building floor, the high-frequency vibration velocity gradually decreased. This tendency was evident in the z-direction. There were multiple peaks in the vibration velocity of each direction with the frequency band distribution. Therefore, in the evaluation standard system of building safety based on vibration velocity and frequency, the natural frequency of the building should be used as a reference to select the corresponding main vibration frequency band or the particle velocity close to its resonance frequency band to evaluate the safety of buildings.

4.2.3. Analysis of Total Vibration Energy of Different Floors. The energy value of the mass element considering each floor as the unit mass was calculated by wavelet packet transform. In order to characterize the response relationship of each

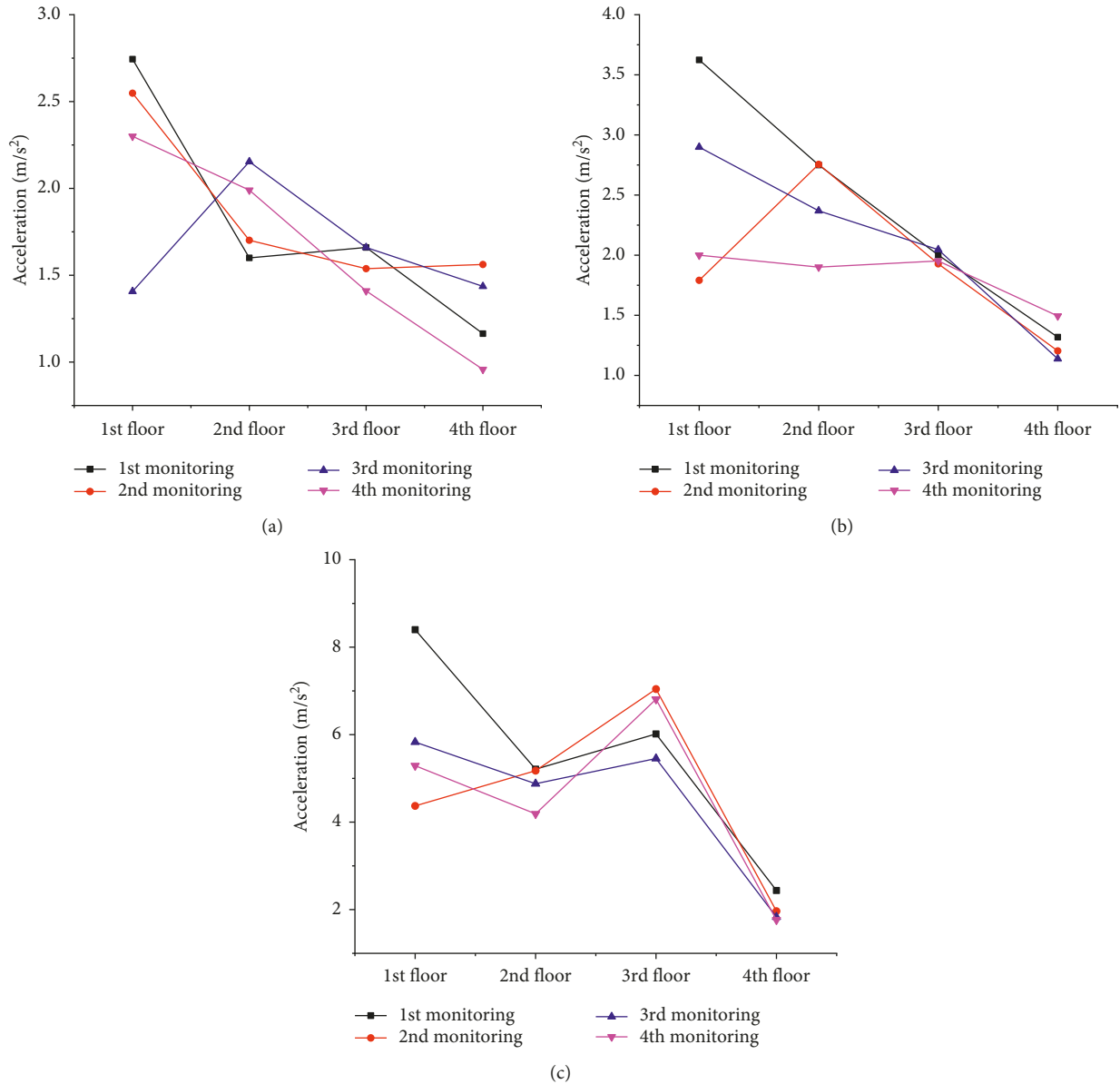


FIGURE 10: Maximum acceleration: (a)  $x$ ; (b)  $y$ ; (c)  $z$ .

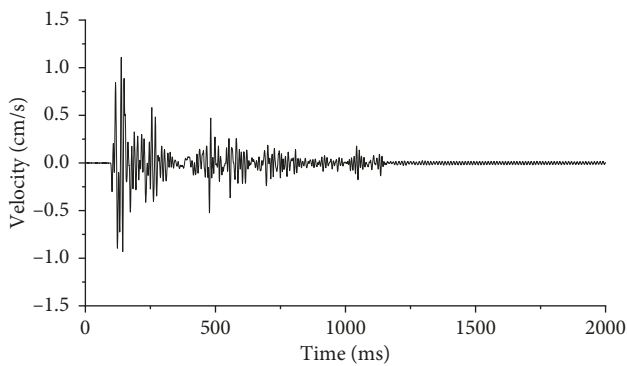


FIGURE 11: Particle velocity in the  $z$ -direction at the first layer in the third monitoring.

floor to the blasting vibration more comprehensively, the energy values by the  $x$ ,  $y$ , and  $z$  vibrations at each floor were added to obtain the total energy value of each floor in response to the blasting vibration.

It can be seen from Figure 15 that the total energy value of vibration increased to the 3rd floor and then decreased to the 4th floor with increasing the building floor. However, the total energy value of the 4th floor was still larger than that of the 1st and 2nd floors. It indicates that the higher the floor, the more affected the blasting vibration, and the more vulnerable it is to destroy.

4.2.4. *Vibration Energy with respect to the Frequency Band.* Based on MATLAB software, the wavelet analysis calculation program of vibration signal was used to calculate the

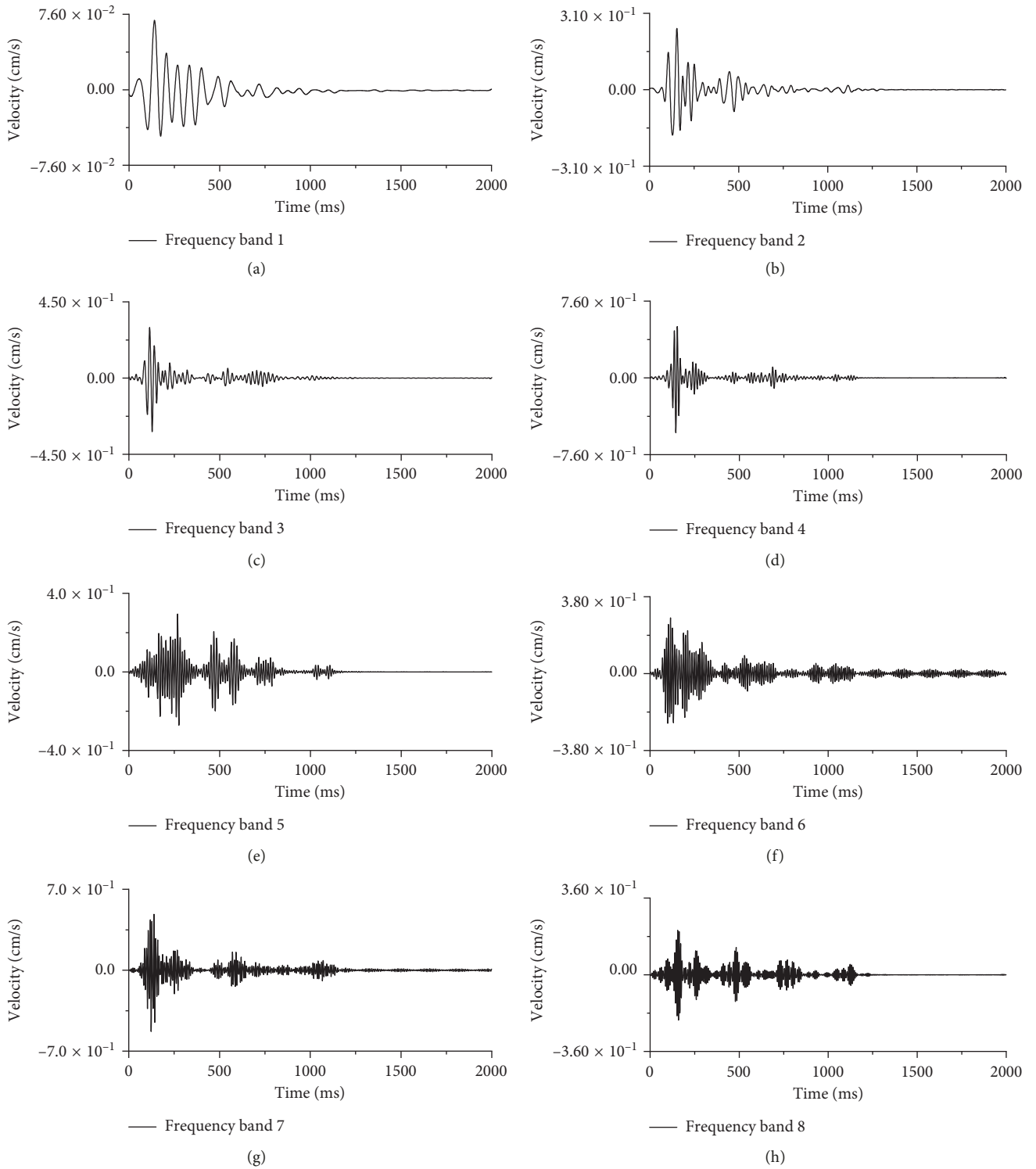


FIGURE 12: Continued.

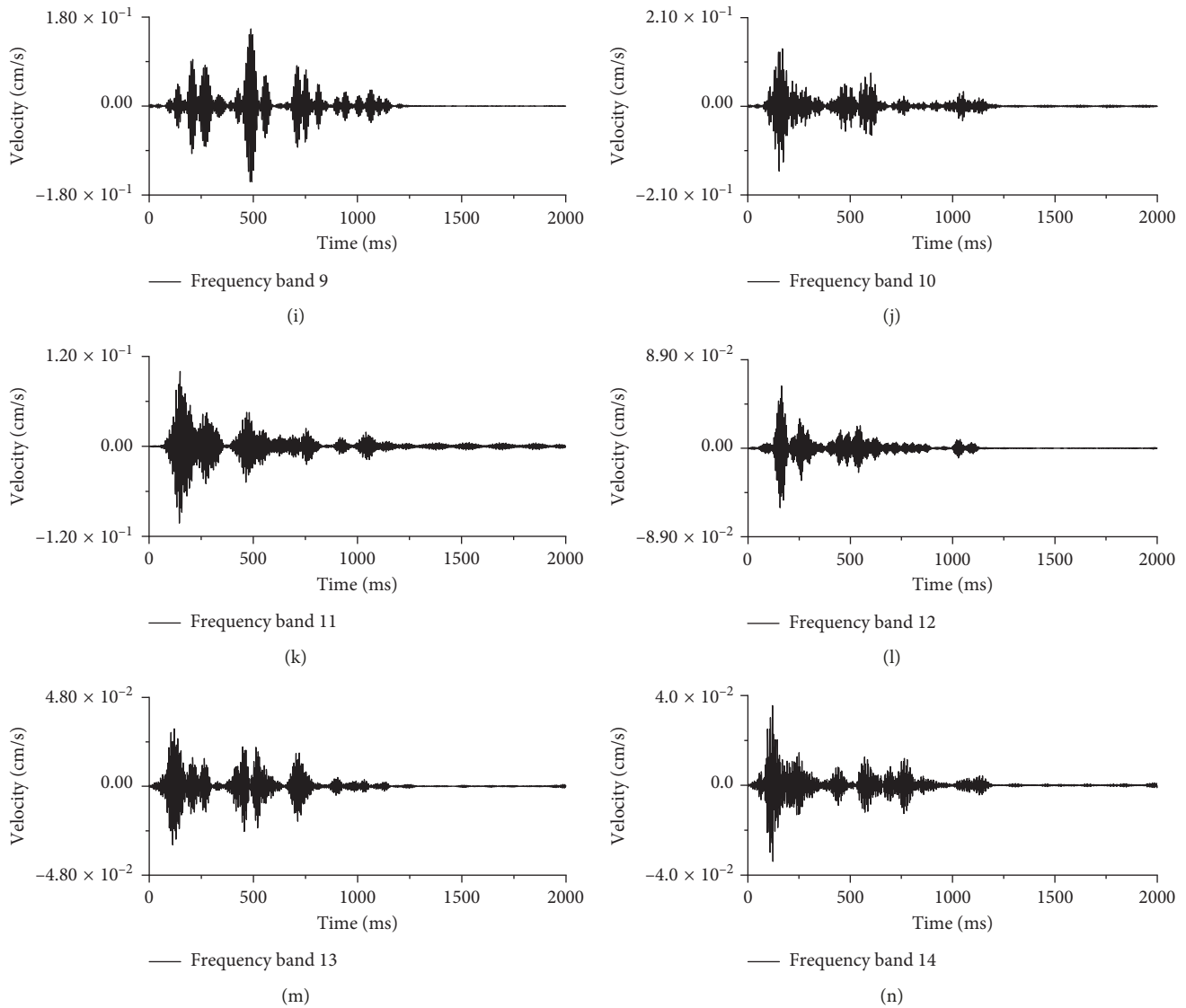
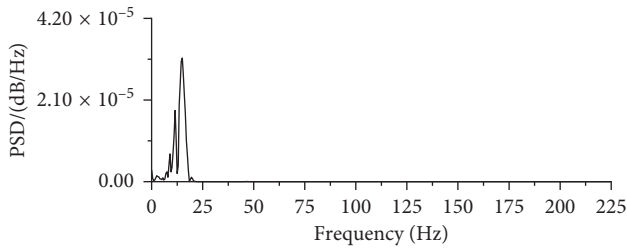


FIGURE 12: Wavelet packet decomposition results for the wave in Figure 11 (frequency bands 1~14).

energy of each frequency band signal. The relationship between the vibration energy value and the energy percentage in the  $z$ -direction of each floor is shown in Figure 16. The energy of the building's response to the blasting vibration was between 0 and 171.6 Hz. The higher the floor was, the more concentrated in the frequency domain of the low frequency the energy was. For buildings with a low natural frequency, the lowering of the response frequency means that it approaches to the building's natural frequency and more likely it causes resonance in the building.

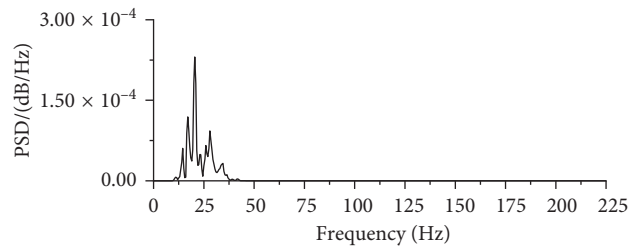
Based on the propagation characteristics of the vibration wave in the medium, previous literature [23, 24] have concluded in similar projects that the main vibration frequency, duration, and acceleration of the buildings decreased with the increase in the number of floors, which was consistent with the conclusions in this paper (Figures 8–10).

Besides, their conclusions also believed that the maximum particle velocity increased with the increase in the number of floor, which was different from the conclusion here. The mechanisms of buildings to blasting vibration is very complex, which depends not only on the characteristics of vibration load (amplitude, frequency, etc.), but also on the natural frequency and damping properties of buildings [25]. The buildings in this paper have several significant features: (1) Compared with the amount of small stone blocks and large concrete used for the walls in the 3rd and 4th floors, larger stone blocks and less concrete were used for the walls in the 1st and 2nd floors. (2) The 1st and 2nd floors of the house were built by the mountain without the back wall. (3) Compared with the 1st and 2nd floors, the 3rd and 4th floors were built later, the construction technology and equipment were more mature and advanced, and the overall integrity of



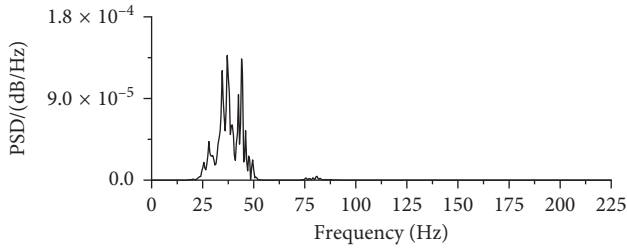
— Frequency band 1

(a)



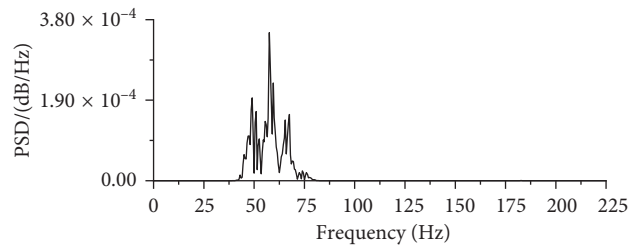
— Frequency band 2

(b)



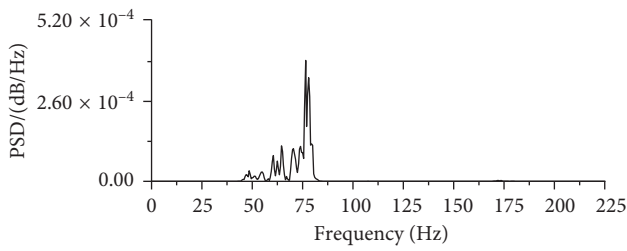
— Frequency band 3

(c)



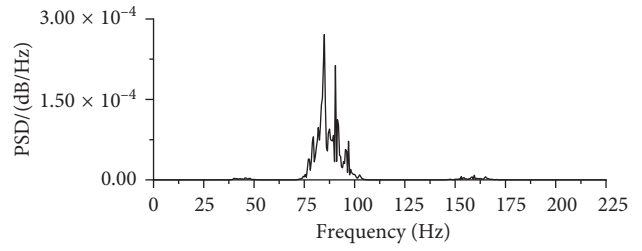
— Frequency band 4

(d)



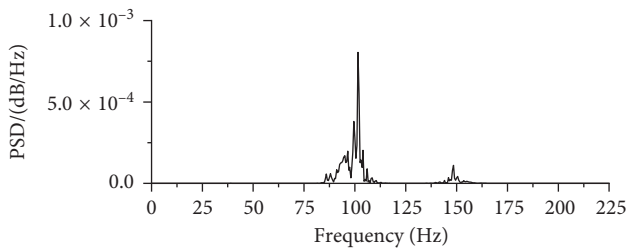
— Frequency band 5

(e)



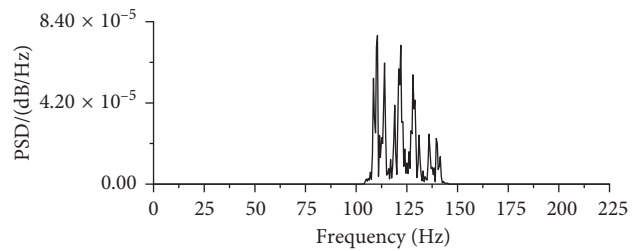
— Frequency band 6

(f)



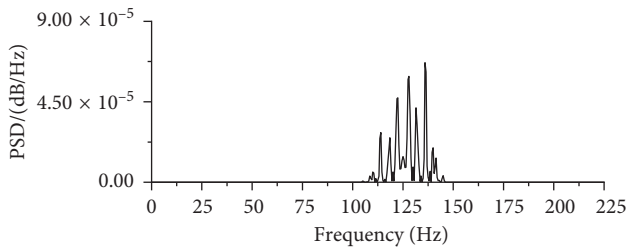
— Frequency band 7

(g)



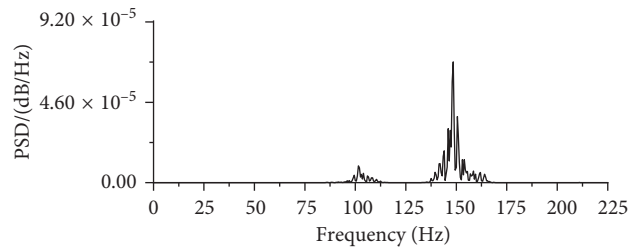
— Frequency band 8

(h)



— Frequency band 9

(i)



— Frequency band 10

(j)

FIGURE 13: Continued.

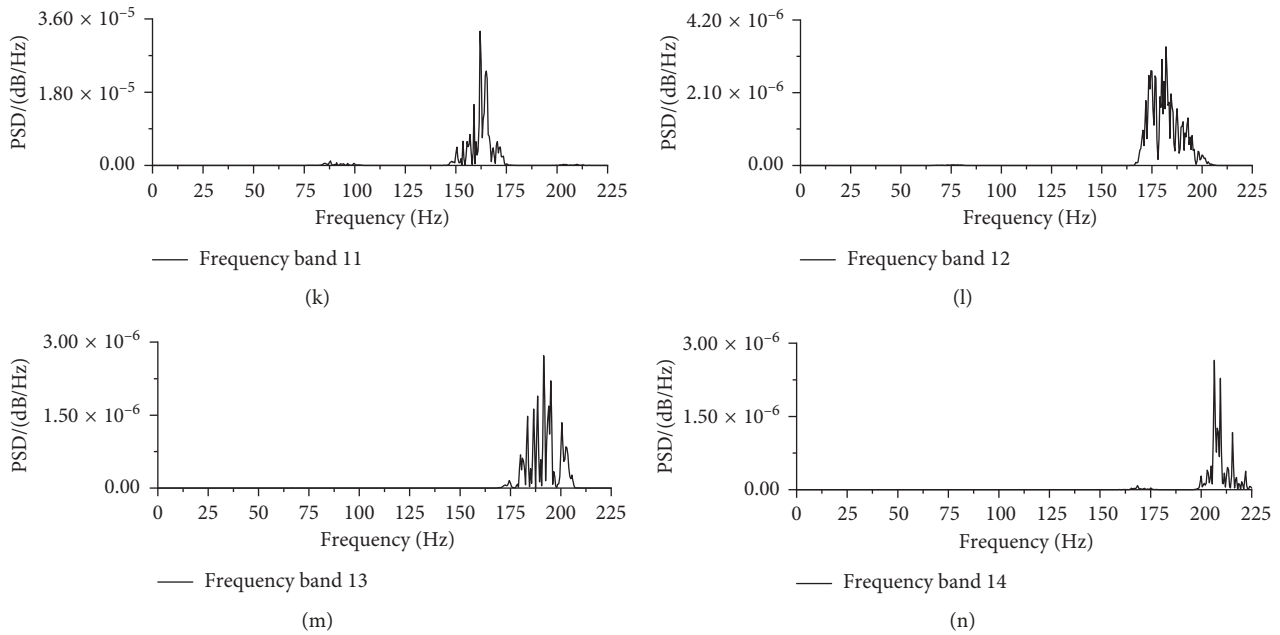


FIGURE 13: The power spectral density for the wave in Figure 11 (frequency bands 1~14).

TABLE 3: Main frequency domain and dominant frequency data.

Floor	1st	2nd	3rd	4th
Main frequency domain (Hz)	14.6~109.2	14.6~140.4	14.6~78	14.6~46.8
Frequency band 1	15	13.5	14	14
Frequency band 2	20.5	28	28.5	28.5
Frequency band 3	37	40	44	32.5
Frequency band 4	57.5	47	50	49.5
Frequency band 5	76.5	67.5	73.5	74.5
Frequency band 6	85	89.5	82	79
Frequency band 7	101.5	101.5	104	102
Frequency band 8	110.5	119	113.5	113.5
Frequency band 9	136	128	132	127.5
Frequency band 10	148.5	151.5	148	148
Frequency band 11	162	159.5	156.5	160.5
Frequency band 12	182	177	174.5	173.5
Frequency band 13	191.5	192	192.5	200.5
Frequency band 14	206.5	206	212	217

the building was better. Clearly, the 3rd and 4th layers have smaller stiffness, stronger strength, and more uniform mass and stiffness distribution than the 1st and 2nd layers.

The building selectively amplifies and suppresses vibration waves transmitted from the foundation [26]. The harmonic could be amplified when its natural period is close to that of the building. Otherwise, the harmonic will be absorbed. After the vibration wave transmitted to the building, the harmonics similar to the natural period of the material used in the 1st and 2nd layers of the building were amplified, and the harmonics with significant differences were absorbed. Due to the difference of materials between the upper two layers and the lower two layers, the natural periods

of them were different. When the vibration wave transmitted to the 3rd and 4th layers, the harmonics amplified in the 1st and 2nd layers might be suppressed in the 3rd and 4th layers. This can be well reflected from the distribution of peak particle velocity with frequency (Figure 14), the peak particle velocity shifted to the low-frequency band with the increasing floor. In addition, a large amount of concrete in the 3rd and 4th floors of the building means larger concrete interlayer in the stone wall than the lower two layers, which has an inhibitory effect on the propagation of vibration waves. The above comprehensive factors lead to increasing peak particle velocity and total energy of the building in 1–3 layers and decreasing in 3–4 layers (Figures 7 and 15).

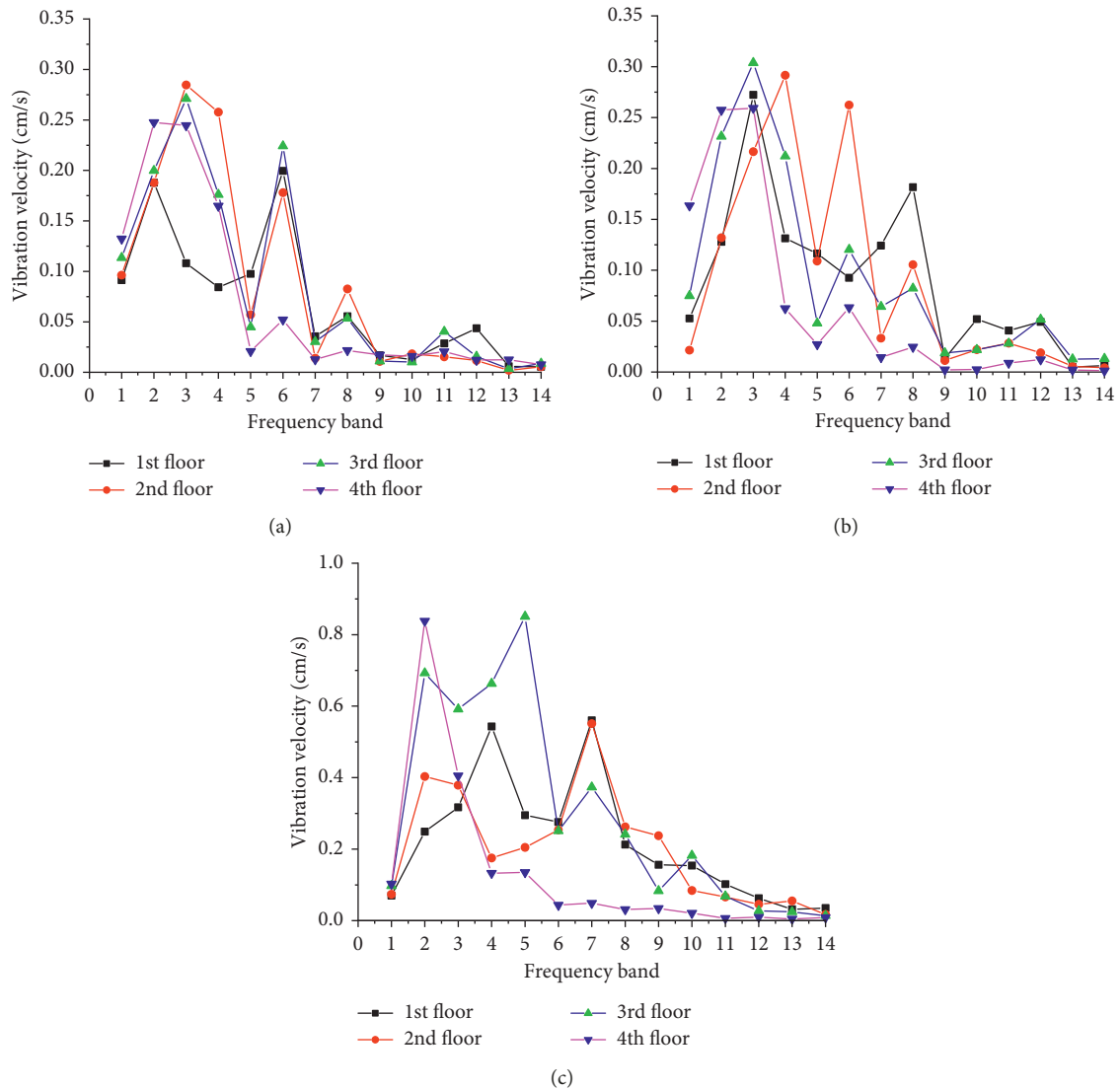


FIGURE 14: Distribution of maximum particle velocity with respect to the frequency band in three directions of  $x$  (a),  $y$  (b), and  $z$  (c).

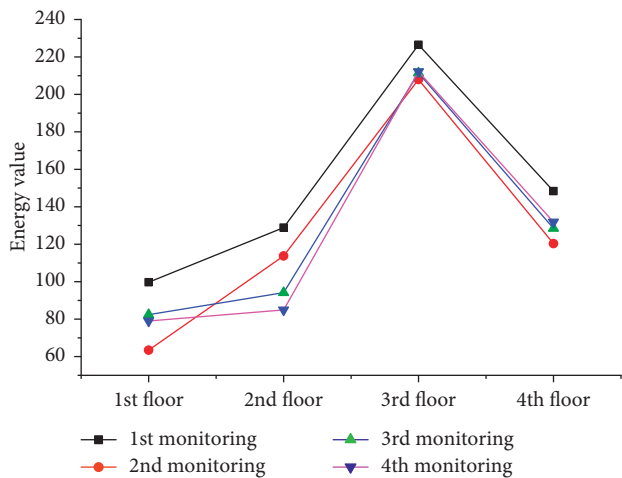


FIGURE 15: Total energy distribution of vibrations on different floors.

### 5. Conclusions

This paper studied the response of multistory building structure to tunnel blasting for the case of the Dizong tunnel. Combined with the on-site monitoring data, wavelet packet analysis technology based on MATLAB programming was used. The following conclusions can be drawn.

The maximum particle velocity increased to the 3rd floor; attenuation occurred in the 4th floor. The particle velocity in the  $z$ -direction was the largest, and it should be paid attention. The dominant frequency of the building showed a trend from high frequency to low frequency, the duration became short and the acceleration decreased to the 4th floor.

The dominant frequency domain of the building became smaller and gradually concentrated to the low-frequency domain to the 4th floor. The response signal of the building to the blasting vibration was widely distributed in the

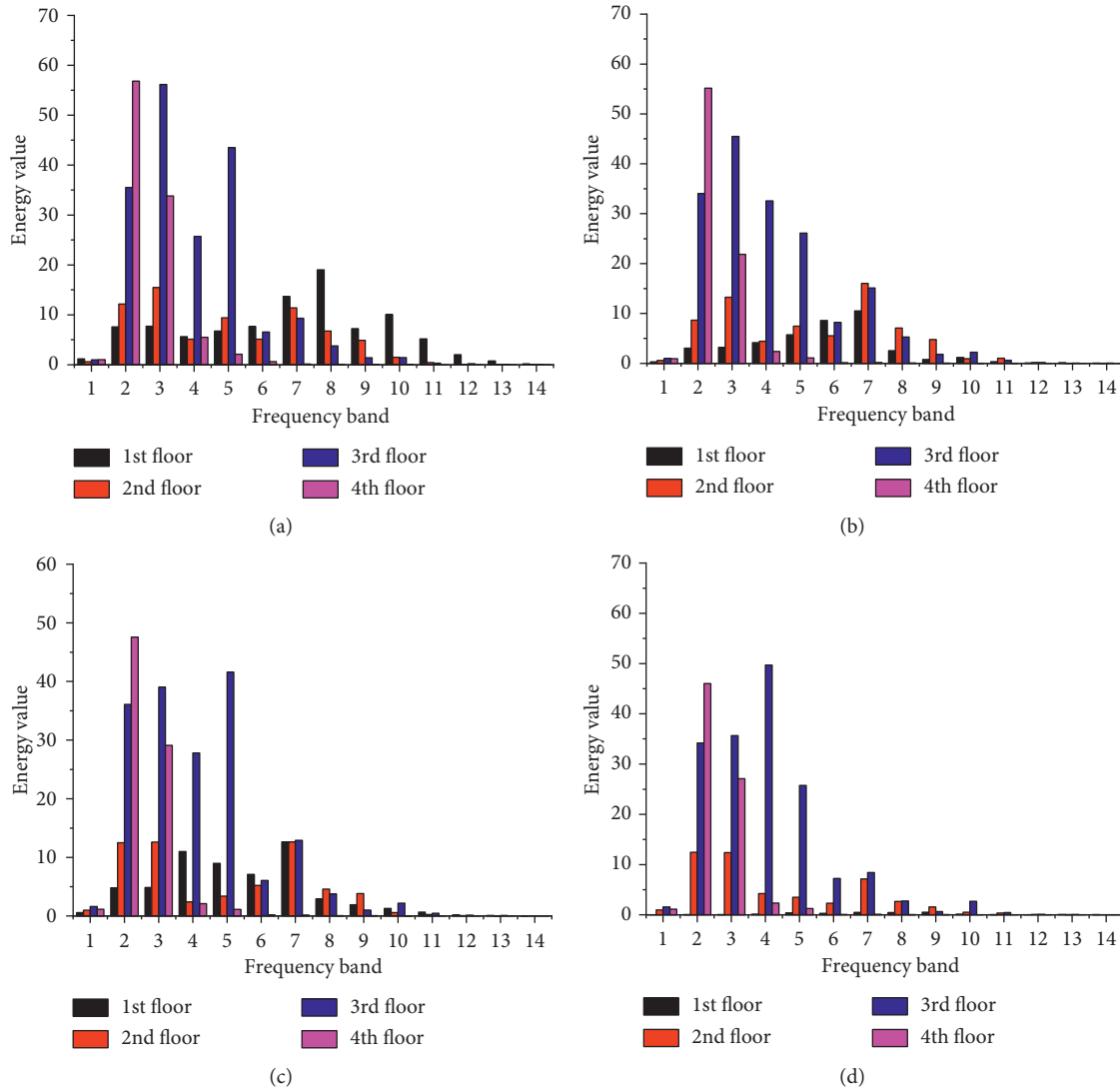


FIGURE 16: The energy of vibration in the z-direction in the (a) 1st, (b) 2nd, (c) 3rd, and (d) 4th floor.

frequency domain, but its main frequency band was basically between 0 and ~140 Hz.

With the increase in the building floor, the high-frequency particle velocity gradually decreased, gathered to the low frequency, and developed from the dispersed multiband to the concentrated low-frequency band. This trend was evident in the z-direction. There were multiple peaks in the vibration velocity of each direction with the frequency band distribution, and the frequency domain corresponding to the peak was dispersed.

The energy of the building’s response to the blasting vibration was between 0 and 171.6 Hz. The frequency domain corresponding to the dominant energy generated by the vibration of the building developed to the low frequency. Moreover, the higher the floor, the higher the low-frequency energy, the more concentrated for the frequency domain of the low frequency. In the low-frequency band, not only the energy value but also the energy increased toward the low frequency.

### Data Availability

The data used to support the findings of this study are available from the corresponding author upon request.

### Conflicts of Interest

The authors declare that they have no conflicts of interest.

### Acknowledgments

The authors would like to thank the National Natural Science Foundation of China (51578447 and 41172237) for supporting this research project.

### References

[1] C. H. Dowding, C. T. Aimone-Martin, B. M. Meins, and E. Hamdi, “Large structure response to high frequency

- excitation from rock blasting,” *International Journal of Rock Mechanics and Mining Sciences*, vol. 111, pp. 54–63, 2018.
- [2] H. Ma, H. Wang, C. He, Z. Zhang, and X. Ma, “Influences of blasting sequence on the vibration velocity of surface particles: a case study of Qingdao metro, China,” *Geotechnical and Geological Engineering*, vol. 35, no. 1, pp. 485–492, 2016.
  - [3] J. H. Yang, W. B. Lu, Q. H. Jiang, C. Yao, and C. B. Zhou, “Frequency comparison of blast-induced vibration per delay for the full-face millisecond delay blasting in underground opening excavation,” *Tunnelling and Underground Space Technology*, vol. 51, pp. 189–201, 2016.
  - [4] X. Qiao, J.-x. Chen, M.-s. Wang et al., “Experimental analysis of influence of blasting vibration in a hydraulic tunnel on surrounding buildings,” *China Earthquake Engineering Journal*, vol. 38, no. 4, pp. 504–509, 2016.
  - [5] S.-d. Yuan, L. Yang, and J. Huang, “Scope affected by metro tunnel construction blasting in Qingdao,” *Modern Tunnelling Technology*, vol. 55, no. 3, pp. 76–80, 2018.
  - [6] L. Wang and H.-l. Wang, “Influence of different direction vibration peak velocity of tunnel blasting on building,” *Blasting*, vol. 29, no. 4, pp. 6–9, 2012.
  - [7] R. Nateghi, “Prediction of ground vibration level induced by blasting at different rock units,” *International Journal of Rock Mechanics and Mining Sciences*, vol. 48, no. 6, pp. 899–908, 2011.
  - [8] H. Fan, D. Yu, D. Zhao, J. Lai, and Y. Xie, “Experimental and numerical investigation of blasting-induced ground vibration from tunnel undercrossing a village,” *Stavebni obzor-Civil Engineering Journal*, vol. 26, no. 4, pp. 404–417, 2017.
  - [9] J.-H. Shin, H.-G. Moon, and S.-E. Chae, “Effect of blast-induced vibration on existing tunnels in soft rocks,” *Tunnelling and Underground Space Technology*, vol. 26, no. 1, pp. 51–61, 2011.
  - [10] B. Duan, H. Xia, and X. Yang, “Impacts of bench blasting vibration on the stability of the surrounding rock masses of roadways,” *Tunnelling and Underground Space Technology*, vol. 71, pp. 605–622, 2018.
  - [11] V. K. Dang, D. Dias, N. A. Do et al., “Impact of blasting at tunnel face on an existing adjacent tunnel,” *International Journal of Geomate*, vol. 15, no. 47, pp. 22–31, 2018.
  - [12] N. E. Rebello, R. Shivashankar, and V. R. Sastry, “Response of strata and buildings to blast induced vibrations in the presence and absence of a tunnel,” *Geotechnical and Geological Engineering*, vol. 34, no. 4, pp. 1013–1028, 2016.
  - [13] D.-y. Li and T. Wang, “Experimental and numerical analysis on influence of blasting in shallow tunnel excavation on surface buildings,” *Journal of Safety Science and Technology*, vol. 11, no. 11, pp. 112–117, 2015.
  - [14] C. Zhang, “Research on the response law of surface particle for shallow buried tunnel blasting vibration,” *Highway*, vol. 10, pp. 246–250, 2016.
  - [15] Z.-x. Chen, B.-w. Hu, and Y.-b. Liu, “Research on vibration and antivibration which blasting vibration imposed on building near to tunnel,” *Earthquake Resistant Engineering and Retrofitting*, vol. 34, no. 4, pp. 73–75, 2012.
  - [16] X.-m. Guan, H.-x. Fu, and M.-s. Wang, “Blasting vibration characteristics monitoring of tunnel under-passing hillside buildings in short-distance,” *Rock and Soil Mechanics*, vol. 7, pp. 1995–2003, 2014.
  - [17] Z.-w. Wang, X.-b. Li, K. Peng, and J.-f. Xie, “Impact of blasting parameters on vibration signal spectrum: determination and statistical evidence,” *Tunnelling and Underground Space Technology*, vol. 48, pp. 94–100, 2015.
  - [18] M.-t. Liu and Q.-s. Chen, “Characteristics of building structure dynamic response to blasting earthquake,” *Blasting*, vol. 4, pp. 23–28, 2005.
  - [19] GB6722-2014, *Safety Regulations for Blasting*, Standards Press of China, Beijing, China, 2014.
  - [20] X. Li, J. Ma, H.-y. Li et al., “Analysis of vibration effects to deep and thick silt by blasting compaction,” *Hydro-Science and engineering*, vol. 1, pp. 71–77, 2016.
  - [21] T.-h. Ling and X.-b. Li, “The features of energy distribution for blast vibration signals in underground engineering by wavelet packet analysis,” *Explosion and shock waves*, vol. 1, pp. 63–68, 2004.
  - [22] T.-h. Ling, *Blast Vibration Effect and Initiative Control of Vibration Damage*, Central South University, Changsha, China, 2004.
  - [23] Q. Zheng, C.-m. Lin, L.-q. Lin et al., “Effect of small-distance tunnel blasting on hilltop stone building vibration,” *Journal of Huaqiao University (Natural Science)*, vol. 32, no. 1, pp. 81–86, 2011.
  - [24] J. Lin, C.-m. Lin, and L.-q. Lin, “Research on characteristics of the structure’s response under the dynamic blasting load,” *Journal of Vibration and Shock*, vol. 29, no. 3, pp. 48–51, 2010.
  - [25] R. P. Dhakal and T.-C. Pan, “Response characteristics of structures subjected to blasting-induced ground motion,” *International journal of Impact Engineering*, vol. 28, no. 8, pp. 813–828, 2003.
  - [26] D. E. Siskind, *Structure response and damage produced by ground vibration from surface mine blasting*, US Department of the Interior, Bureau of Mines, New York, NY, USA, 1980.



Hindawi

Submit your manuscripts at  
[www.hindawi.com](http://www.hindawi.com)

